

Ovalbumin Delivery by Guanidine-Terminated Dendrimers Bearing an Amyloid-Promoting Peptide via Nanoparticle Formulation

Chie Kojima,^{*,†} Rina Kameyama,[‡] Manami Yamada,[‡] Masahiro Ichikawa,[‡] Tomonori Waku,[‡] Akihiro Handa,[§] and Naoki Tanaka^{*,‡}

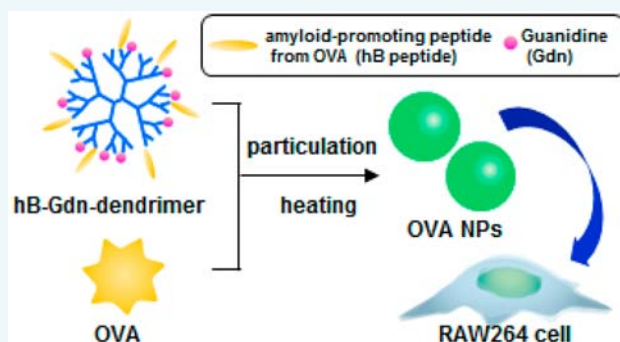
[†]Department of Applied Chemistry, Graduate School of Engineering, Osaka Prefecture University, 1-2 Gakuen-cho, Naka-ku, Sakai, Osaka 599-8570, Japan

[‡]Faculty of Molecular Chemistry and Engineering, Kyoto Institute of Technology, Goshyokaido-cho, Matsugasaki, Sakyo-ku, Kyoto 606-8585, Japan

[§]R&D Division, Kewpie Corporation, 2-5-7 Sengawa-cho, Chofu-shi, Tokyo, 182-002, Japan

S Supporting Information

ABSTRACT: Development of protein delivery systems is important for biomedical applications such as immunotherapy. Ovalbumin (OVA) is a major component of egg whites, and is a possible cause of egg allergy. In this study, OVA was used as a model protein to develop a delivery system using guanidine-terminated dendrimers (Gdn-den) bearing an amyloid-promoting peptide derived from the helix B (hB) region of OVA (hB-Gdn-den). OVA nanoparticles (NPs) were prepared by heat treatment of OVA/hB-Gdn-den mixtures. The NP size and the surface charge were controlled by adjusting the ratio of hB-Gdn-den to OVA. The NPs were around 200 nm in diameter and stably dispersed, and their encapsulation efficiency for OVA was more than 80%. Although OVA NPs were also prepared using Gdn-den, the NPs aggregated readily. Complexation with hB-Gdn-den induced conformational changes in the OVA, and the hB peptide promoted digestion of OVA. These suggest that the hB peptide of the Gdn-den works as a possible anchor to OVA. The positively charged OVA NPs effectively associated with RAW264 cells. Thus, the amyloid-promoting Gdn-den, when mixed with OVA at a suitable molar ratio to form NPs, could act as a carrier for delivery of antigen proteins to immune cells.



INTRODUCTION

Proteins have many functions, including as reactors, catalysts, sensors, antibodies, and adaptors. For biomedical applications, delivery of bioactive proteins into cells is required because proteins typically do not internalize into cells on their own, and many studies have investigated protein delivery systems to achieve this.^{1–3} Delivery of antigen proteins (or protein fragments) into immune cells is particularly important for immunotherapy. In cancer immunotherapy, a cancer-specific antigen protein is administered to a patient to activate antigen-specific cytotoxic T lymphocytes and induce damage to cancer cells. Because the body's own immune system is used to destroy cancer cells in cancer immunotherapy, it is more patient-friendly than conventional cancer therapy such as surgery, chemotherapy, and radiotherapy.^{4,5} The addition of cell-penetrating peptides to an antigen protein reportedly improves cell internalization.^{6,7} However, a chemical reaction or recombinant technology is necessary to add the cell-penetrating peptides, and this can affect the function of the original protein. Additionally, the stability of a protein dispersion can decrease with the addition of cell-penetrating peptides. Nanoparticle (NP)-based systems can be used as protein delivery systems,

and the behaviors can be controlled by the size and surface properties of the NPs. However, various types of NPs available, including liposomes, micelles, and nanogels, have relatively low protein loading efficiencies.^{2,3,8} Thus, development of a NP formulation with high protein loading is necessary. Nucleic acids such as DNA and RNA can be complexed with lipids and/or polymers to form NPs. In a similar manner, formation of protein–polymer complexes could produce NPs with high loading efficiency.

Dendrimers are a promising nanoplatform because they have highly controllable sizes and surface properties. In addition, multiple bioactive molecules can be loaded onto a dendrimer because they have many functional groups at the periphery. There have been numerous reports on the application of dendrimers to drug and gene delivery systems.^{9–12} Previously, antigen peptides have been conjugated to dendrimers to produce antigen peptide-conjugated dendrimers. Protein model peptides and some ligand peptides have also been conjugated to

Received: June 9, 2015

Revised: July 14, 2015

Published: July 17, 2015



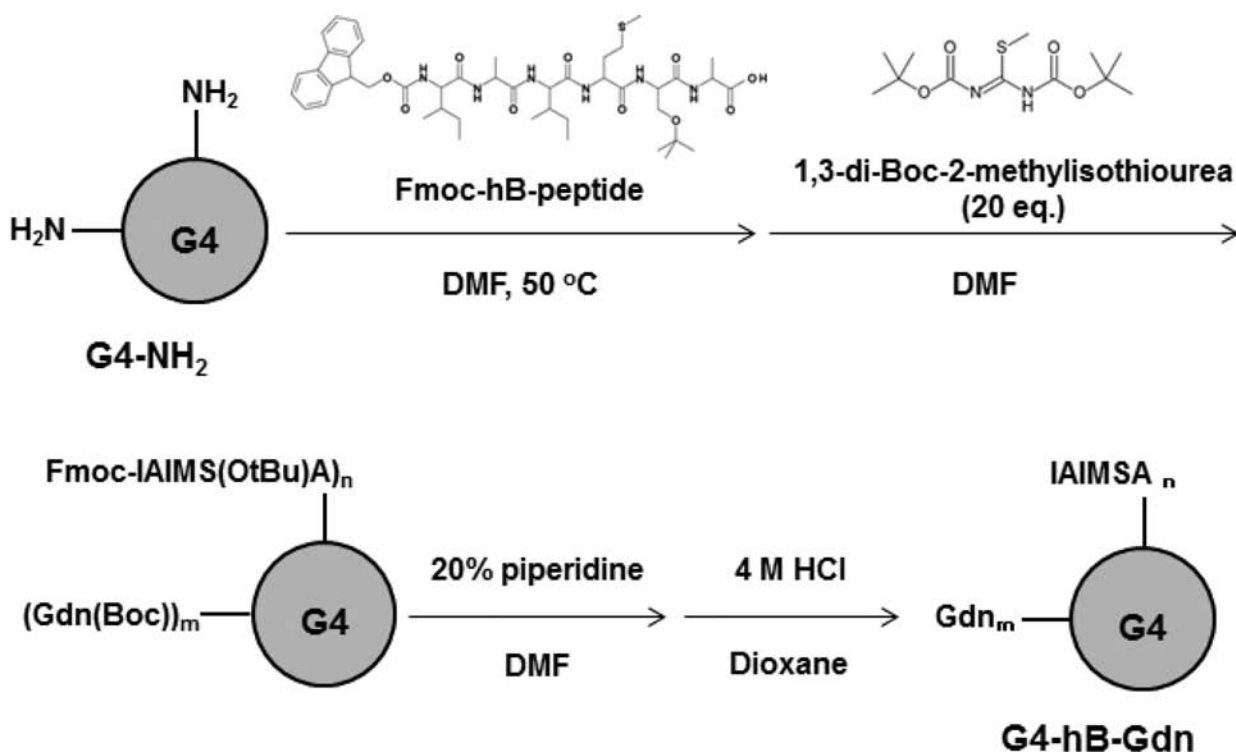


Figure 1. Synthetic pathway of hB-Gdn-den.

dendrimers.^{11–14} However, to the best of our knowledge, only one paper has been published on protein delivery using dendrimers.¹⁵ Conjugation is not suitable for delivery of complete proteins, because proteins and dendrimers have similar molecular weights. Complex formation is more suitable for protein delivery. It has been reported that guanidine-terminated dendrimers (Gdn-den) work as dendritic molecular glues with proteins, with the guanidinium ions forming a salt bridge with oxyanions in the proteins.¹⁶ Guanidine groups at the periphery of dendrimers also enhance cell internalization in gene delivery.^{17,18} Thus, Gdn-den are useful for protein delivery.

Ovalbumin (OVA) is a glycoprotein of 45 kDa with a pI of 4.5. It is a major component of egg whites, and a possible cause of egg allergy. The fragment ²⁵⁷SIINFEKL²⁶⁴ is an epitope that induces undesirable immune reactions. Thus, OVA has been used as a model antigen. Interestingly, it has been reported that OVA forms fibrous aggregates after heat treatment at 80 °C. An earlier study identified some amyloidogenic core regions localized at the helix B (hB) region. The ³²IAIMSA³⁷ fragment was found to promote amyloid formation, and has been named the hB peptide.¹⁹

The aim of this study was to develop a protein delivery system using OVA as a model protein. Following the earlier report on dendritic molecular glue, a Gdn-den was applied to OVA delivery. However, the OVA NP prepared with the Gdn-den aggregated in 1 day. To overcome this, we synthesized a dendrimer containing the guanidino group and hB peptide (hB-Gdn-den) for the OVA NP formulation, and this was named the amyloid-promoting guanidine-terminated dendrimer. hB-Gdn-den and OVA were mixed at different molar ratios, and the subsequent heat treatment of the mixture produced OVA NPs. The size, surface charge, and stability of the dispersion of the OVA NPs were examined. Enzymatic digestion and cell association with macrophages were also investigated. A

dendrimer with the guanidino group but without the hB peptide (Gdn-den) was also synthesized, and the properties of the OVA NPs prepared with this dendrimer were compared with those of the NPs from hB-Gdn-den.

RESULTS AND DISCUSSION

Synthesis of hB-Gdn-den. First, hB-Gdn-den was synthesized as shown in Figure 1. Fluorenylmethyloxycarbonyl (Fmoc)-protected amyloid-promoting peptide (Fmoc-hB-peptide, Fmoc-IAIMS(O^tBu)A) was conjugated to a polyamido-amine (PAMAM) dendrimer of generation 4 (G4). The Fmoc group is commonly used in peptide synthesis because primary amines are insensitive to this group. Fmoc solid-phase peptide synthesis from the amino groups at the dendrimer termini has been previously reported, suggesting that the terminal amino groups do not affect Fmoc groups in the reactants.²⁰ Then, 1,3-di-Boc-2-methylisothiourea was reacted with the Fmoc-hB-peptide-conjugated dendrimer for guanidination of the remaining dendrimer termini. The dendrimers were purified by reprecipitation several times before the next reaction, and the final product was purified by dialysis to remove small compounds, as described in the Experimental Procedures. The NMR spectrum of the Fmoc-hB-peptide- and Boc-Gdn-conjugated dendrimer showed signals derived from the dendrimer (2.2 ppm), Fmoc-hB-peptide (1.1 ppm), and Boc-Gdn (1.4 ppm). From the ratios of these signals, it was estimated that three Fmoc-hB-peptides and 15 Boc-Gdn were conjugated to the dendrimer. Because the PAMAM G4 dendrimer contains 64 amino termini, the remaining 46 terminal groups are amino groups. After deprotection, the NMR signals of Boc (1.4 ppm) and Fmoc (7.3 and 7.9 ppm) disappeared, indicating that these protective groups were removed, leaving hB-Gdn-den (Figure 2). The OtBu group on the side chain of serine in the hB peptide was also deprotected. However, from the corresponding signal at 1.1

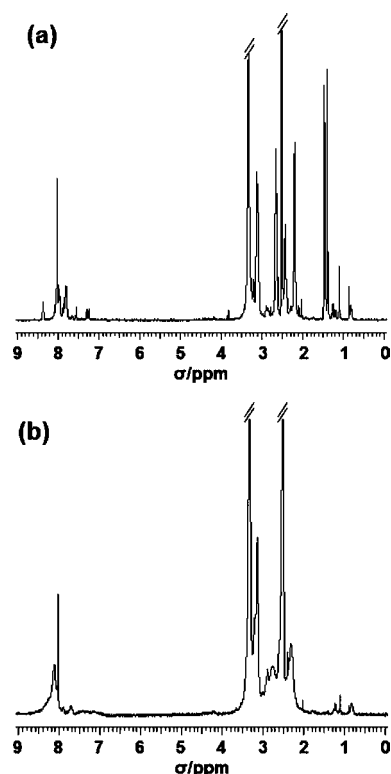


Figure 2. NMR spectra of the Fmoc-hB-peptide/Boc-Gdn-conjugated dendrimer (a) and hB-Gdn-den (b).

ppm in the NMR spectra, it was estimated that half of these groups remained protected. As a control, a Gdn-den without the hB peptide was also synthesized. From the NMR spectrum, it was estimated that 62 termini of the G4 PAMAM dendrimer were converted from amino groups to guanidino groups (Figure S1).

Preparation of OVA NPs Using hB-Gdn-den at Different Molar Ratios. To prepare the OVA NPs, hB-Gdn-den was mixed with OVA at hB-Gdn-den to OVA molar ratios of between 0.25 and 4, and then heated. At all molar ratios, except for 0.5 and 1, NPs with diameters of around 200 nm were observed in the transmission electron microscopy (TEM) images (Figure 3). At the ratios of 0.5 and 1, large aggregates were observed. Without heating, no NPs were observed (Figure S2), indicating that the heat treatment is necessary for formation of OVA NPs. Dynamic light scattering (DLS) analysis showed similar phenomena to the TEM observations. At all molar ratios, except 0.5 and 1, the diameters of the OVA NPs were hundreds of nanometers. For the molar ratios of 0.5 and 1, the OVA NP diameters were on the order of micrometers (Figure 4a). ζ -Potential analysis showed that the NPs formed at the lowest molar ratio were negatively charged, and the ζ -potential increased as the hB-Gdn-den concentration increased (Figure 4b). Because OVA is anionic and hB-Gdn-den is cationic, addition of hB-Gdn-den resulted in a positive shift in the charge. When the molar ratio was 0.5 or 1, the net charge was almost canceled, and suppression of electrostatic repulsion at these molar ratios led to formation of large aggregates. The NPs formed at molar ratios of 0.25 and 2 were used as anionic and cationic OVA NPs in the following assay.

As a control, OVA NPs were also prepared using Gdn-den without the hB peptides. In this case, the NP diameter was

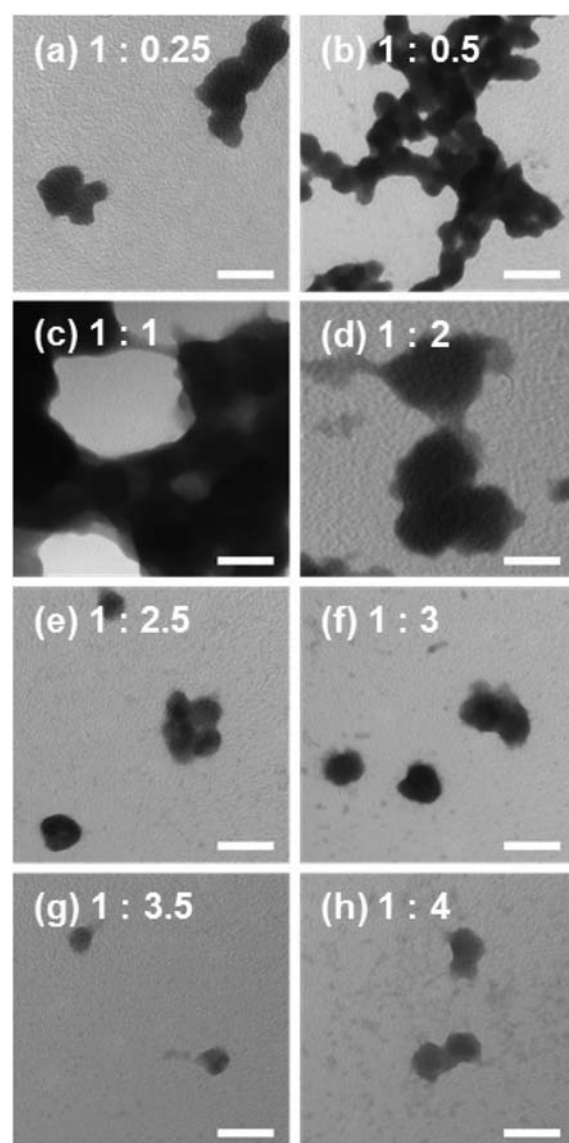


Figure 3. TEM images of the OVA NPs prepared using hB-Gdn-den at different molar ratios. The white bar in the images represents 200 nm.

around 100 nm with molar ratios of 0.25 and 2 (Figure S3). In a similar manner to the OVA/hB-Gdn-den NPs, the ζ -potential increased as the concentration of Gdn-den increased (Figure S4). However, the OVA NPs prepared using Gdn-den were not as stable as those prepared with hB-Gdn-den, and they started to aggregate after only 1 day. By day 3, large aggregates had formed (Figure 5). It has been reported that Gdn-den induces aggregation of anionic proteins such as insulin,²¹ which is consistent with our results. This occurs because cationic Gdn-den functions as a cross-linker with anionic proteins through electrostatic interactions. Regulation of the surface charge on the dendrimer is a possible solution to suppress aggregation. Because the dendrimer charge also affects complex formation for the NP formulation, fine-tuning of the dendrimer charge is necessary to allow for NP formation but suppress aggregation. By contrast, the OVA/hB-Gdn-den NPs remained stably dispersed for a week (Figure 5). Therefore, the hB peptide conjugated to the dendrimer plays an important role in

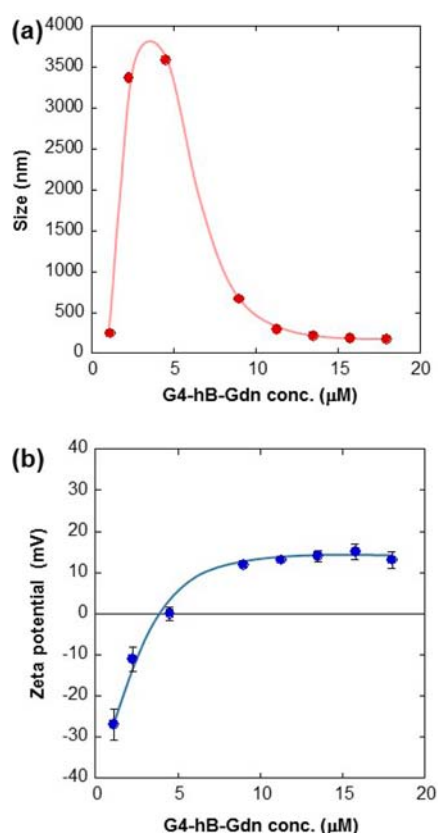


Figure 4. DLS (a) and ζ -potential (b) analyses of the OVA NPs prepared using hB-Gdn-den at different concentrations. [OVA] = 4.5 μ M.

stabilization of the NPs. Consequently, further analysis was performed on the OVA NPs prepared using hB-Gdn-den.

The encapsulation efficiency in an NP is important in NP-based protein delivery systems. In the present study, the OVA NPs were collected by centrifugation, and OVA remaining in the supernatant was detected using a gel permeation chromatography assay. By subtracting the residual OVA from the total OVA, the quantity of OVA loaded on the NPs was estimated. This calculation showed that more than 80% of the OVA was incorporated into the NPs (Table 1). The encapsulation efficiency of the dendrimer in the NPs was also estimated. It has been reported that PAMAM dendrimers fluoresce, although the mechanism is unknown.²² hB-Gdn-den also fluoresces at around 450 nm when excited at 380 nm. In the present study, the amount of residual hB-Gdn-den in the supernatant was evaluated by fluorometry. The results indicated that 83% of the hB-Gdn-den was incorporated into the NPs at a molar ratio of 0.25. By contrast, at molar ratios of 2 and 4, only 48% and 13% of the hB-Gdn-den was incorporated into the NPs, respectively (Table 1). This suggests that free dendrimers will coexist with the OVA NPs at high molar ratios.

Influence of Amyloid-Promoting Peptides in the Dendrimer on OVA. Circular dichroism (CD) spectra of intact OVA, the OVA/dendrimer polyion complexes (before heating) and the OVA NPs (after heating) were measured to investigate whether the dendrimer affected the secondary structure of OVA (Figure 6). Interestingly, the CD patterns of the complex and the NPs prepared using hB-Gdn-den were drastically different from intact OVA, but those for complexes and NPs prepared using Gdn-den were similar. This indicates

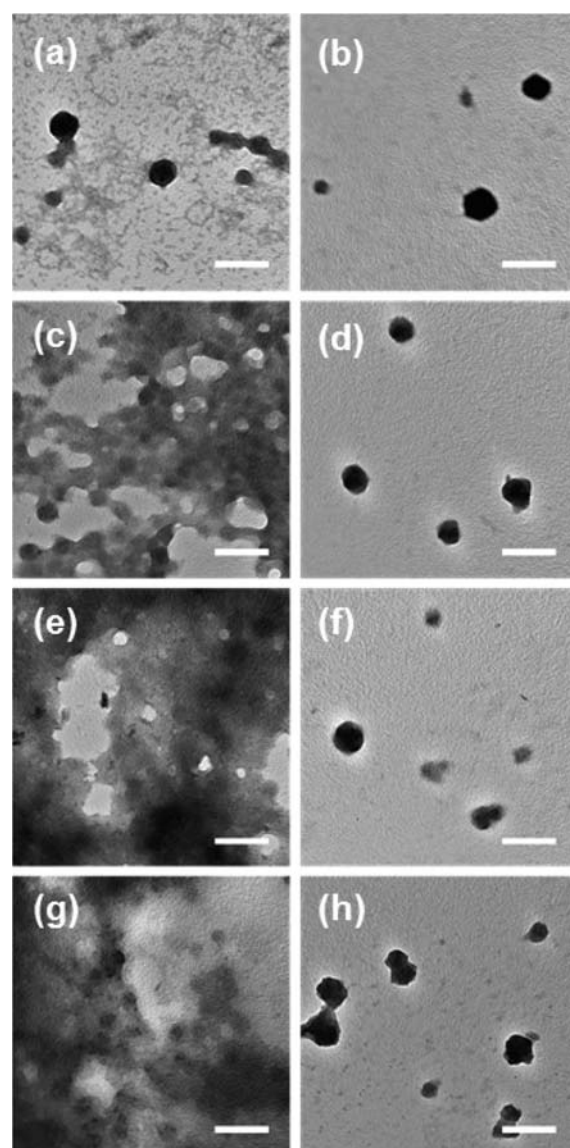


Figure 5. (a) TEM images of the OVA NPs prepared using Gdn-den (a, c, e, and g) and hB-Gdn-den (b, d, f, and h) at a molar ratio of 2 after 1 day (a and b), 3 days (c and d), 5 days (e and f), and 7 days (g and h) at 37 °C. The white bar in the images represents 200 nm.

Table 1. Encapsulation Efficiency of OVA and the Dendrimer in the NPs

molar ratio (hB-Gdn-den/OVA)	OVA (%)	hB-Gdn-den (%)
0.25	80	83
2	93	48
4	93	13

that the hB peptide conjugated to the dendrimer largely affects the secondary structure of OVA and induces conformational changes. This result suggests that the hB peptides conjugated to the dendrimer work as an anchor to OVA, and this would contribute to the stability of the NP formulation and conformational changes.

Digestion of antigen proteins is required for antigen presentation. In the present study, trypsin treatment was performed as a model digestion (Figure 7). A band at 45 kDa was observed after trypsin treatment of intact OVA, and this corresponded to the molecular weight of the native OVA. After

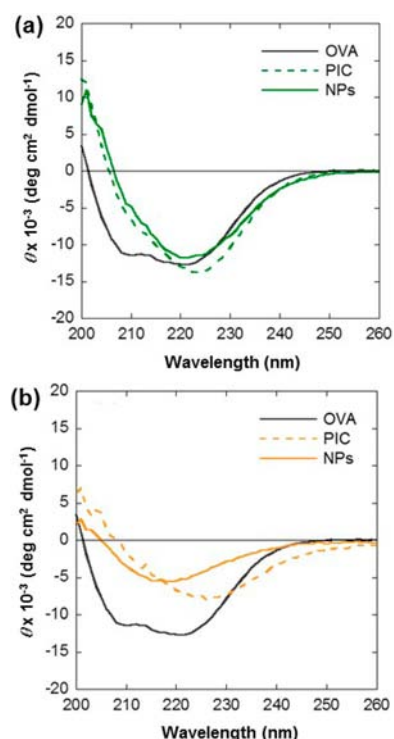


Figure 6. CD spectra of the OVA NPs prepared using Gdn-den (a) and hB-Gdn-den (b) at a molar ratio of 2. Intact OVA and the polyion complex (PIC) were also analyzed.

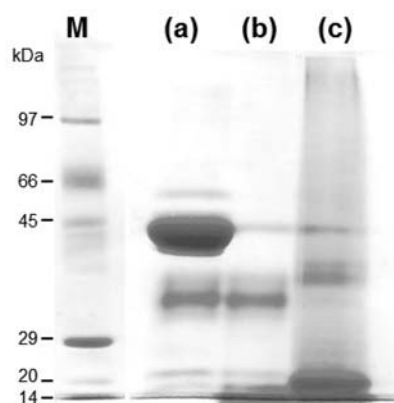


Figure 7. SDS-PAGE of the intact OVA (a), heat denatured OVA (b), and the OVA NPs prepared using hB-Gdn-den (c) at a molar ratio of 2 after treatment with trypsin. M indicates the marker.

heat denaturation, the OVA formed aggregates.¹⁹ The 45 kDa band of the denatured OVA decreased, indicating that the denatured OVA was degraded. The OVA NP prepared using hB-Gdn-den also showed degradation bands, suggesting that the hB-Gdn-den did not interfere with digestion of the antigen protein. Small fragments of less than 20 kDa were dominant for the OVA NP prepared using hB-Gdn-den, while large fragments were observed for the denatured OVA. The OVA NPs prepared using Gdn-den were also treated with trypsin as a control, and large fragments and the intact protein were observed (Figure S5). Because enzyme degradation of the denatured proteins occurs readily, the hB peptide at the dendrimer possibly promoted degradation of OVA.

Cell Association of OVA NPs Prepared Using hB-Gdn-den.

The first step of antigen presentation is association with immune cells such as macrophages. To examine cell association with the OVA NPs, fluorescent dye-labeled OVA (F-OVA) was prepared. The F-OVA NPs prepared using hB-Gdn-den were formed in a similar manner to the nonlabeled OVA NPs (Figure S6). The F-OVA NPs were exposed to mouse-derived macrophage-like cells, RAW264 cells, and the level of cell association was evaluated from microscopic observation. The macrophages treated with F-OVA did not show any large fluorescent signals (Figure 8). Intact OVA was not associated

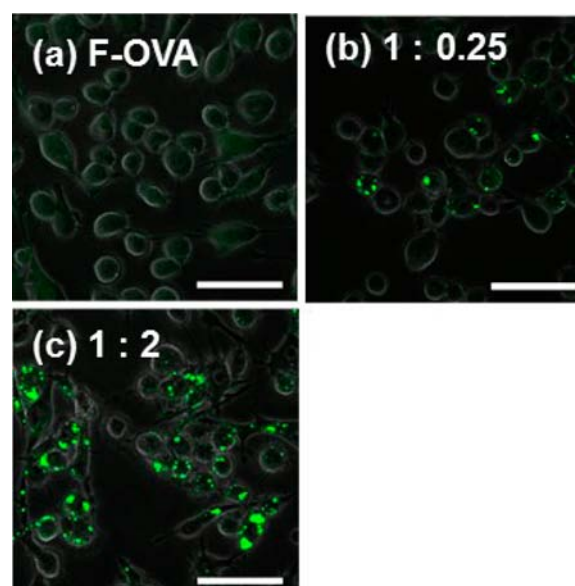


Figure 8. Confocal laser scanning microscope images of RAW264 cells after the 1 h incubation with intact F-OVA and the F-OVA NPs prepared using hB-Gdn-den at different molar ratios. The white bar represents 50 μ m.

with cells. However, the F-OVA NPs exhibited fluorescent signals, which were dependent on the molar ratio. At a molar ratio of 2, more F-OVA NPs were associated with macrophages than at a molar ratio of 0.25. The NPs prepared at these molar ratios were of similar sizes, but they had very different surface charges. The OVA NPs prepared at the higher molar ratio were positive, but those prepared at the lower molar ratio were negative (Figure 4). Because the cell surface is negatively charged, positive NPs can effectively associate with the cell surface through electrostatic interactions. Therefore, the OVA NPs prepared using hB-Gdn-den at high molar ratios will be more useful for delivery into macrophages than OVA NPs prepared at low molar ratios. In our experiments, the cells were treated with trypan blue before the observation to quench the fluorescent dye on the cell surface.²³ Thus, it is likely that the observed fluorescence came from the internalized F-OVA. Intracellular behavior and protein carrier ability of the OVA NPs will be investigated in our future research.

In conclusion, OVA NPs were prepared by mixing OVA with hB-Gdn-den, followed by heat treatment. OVA could be loaded into the NPs with high encapsulation efficiency, and the NP surface charges could be controlled by changing the molar ratio. Positively charged OVA NPs prepared using hB-Gdn-den were stably dispersed and effectively associated with macrophage-like cells. Thus, hB-Gdn-den-based NPs at a suitable molar ratio could be used for delivery of antigen proteins into immune

cells. The guanidinium ions possibly worked as molecular glue and promoted cell association, and the hB peptide possibly worked as an anchor to the OVA. The hB peptide was recognized as an amyloidogenic sequence from protein structure prediction.¹⁹ The *in silico* protein structure prediction suggests that each protein contains its own amyloidogenic sequence.²⁴ It is possible that conjugation of the amyloidogenic peptides to the Gdn-den could provide protein specificity in the NP formulation. Further analyses of this system are ongoing.

■ EXPERIMENTAL PROCEDURES

Materials. Amino-terminated ethylenediamine core PAMAM dendrimer of G4, OVA (98% purity, A5503), 1,3-bis(*tert*-butoxycarbonyl)-2-thiospseudourea (1,3-di-Boc-2-methylisothiourea), and Eagle's minimum essential medium (EMEM) were purchased from Sigma-Aldrich (St. Louis, MO). *o*-(7-Benzotriazol-1-yl)-1,1,3,3-tetramethyluronium hexafluorophosphate, 1-hydroxy-7-benzotriazole, *N,N*-diisopropylethylamine were purchased from Watanabe Chemical Industries Ltd. (Hiroshima, Japan). Fluorescein-4-isothiocyanate was purchased from Dojindo Molecular Technologies, Inc. (Kumamoto, Japan). Fetal bovine serum was purchased from Biowest (Nuaillé, France). Murine macrophage-like RAW264 was obtained from the Riken BRC Cell Bank (Tsukuba, Japan). Fmoc-IAIMS(O^tBu)A was synthesized and purified by Gen-Script (Piscataway, NJ).

Synthesis of hB-Gdn-den. Fmoc-IAIMS(O^tBu)A (11 μ mol) was mixed with 1-hydroxy-7-benzotriazole (11 μ mol), *o*-(7-benzotriazol-1-yl)-1,1,3,3-tetramethyluronium hexafluorophosphate (10 μ mol), and *N,N*-diisopropylethylamine (22 μ mol) in *N,N*-dimethylformamide (DMF). The reaction mixture was added to the G4 PAMAM dendrimer (1.7 μ mol). The resulting solution was stirred at 50 °C for 4 days. After evaporation of the solvent, the residue was washed with diethyl ether. Then, 1,3-bis(*tert*-butoxycarbonyl)-2-thiospseudourea (0.51 mmol) was reacted with the dendrimer in DMF for 3 days. After evaporation of the solvent, the crude compound was purified by reprecipitation from diethyl ether and hexane. Next, the dendrimer was treated with a solution of 20% (volume fraction) piperidine in DMF for 50 min. After evaporation of the solvent, the residue was washed twice with hexane. Then, 4 mol/L HCl-dioxane was treated with the dendrimer for 2.5 h. The crude compound was collected by reprecipitation from acetone and diethyl ether, followed by dialysis in water. The final product (yield 76%) was obtained by freeze-drying.

Synthesis of Gdn-den. Gdn-den was synthesized, as described in an earlier report.²⁵ Briefly, 1,3-bis(*tert*-butoxycarbonyl)-2-thiospseudourea (2.24 mmol) was reacted with the G4 PAMAM dendrimer (7.0 μ mol) in DMF (12 mL) for 3 days. After evaporation of the solvent, the crude compound was purified by reprecipitation from diethyl ether and hexane. Then, 4 mol/L HCl-dioxane was treated with the dendrimer for 2 h at room temperature. The crude compound was collected by reprecipitation from acetone and diethyl ether, followed by dialysis in water. The final product (yield 65%) was obtained by freeze-drying.

Preparation of OVA NPs Using Dendrimers. Equal volumes of an aqueous solution of G4-hB-Gdn or G4-Gdn (1.13–18.0 μ mol/L) and an OVA solution (200 μ g/mL, 4.5 μ mol/L) in 0.5 mmol/L phosphate buffer (pH 7.5) were mixed together. The resulting solution was heated at 80 °C for 30 min, and then stored at 4 °C. For comparison purposes, the

untreated OVA solution was used in experiments as “intact OVA”. “Denatured OVA” was prepared by heat treatment (80 °C, 30 min) of the OVA solution without any dendrimers. Another control, “OVA complex”, was prepared by mixing the OVA solution with the dendrimer solution without heat treatment.

Characterization. The obtained products were characterized by ¹H NMR (JEOL, 600 MHz).

For TEM, the samples were negatively stained with 0.1% phosphotungstate, which was adjusted to pH 7.5 using sodium hydroxide. TEM measurements were performed using a JEM-1200EX II (JEOL, Tokyo, Japan) with an acceleration voltage of 85 keV.

Sample solutions were diluted with phosphate buffer (pH 7.5), with a 2-fold dilution for DLS analysis and a 30-fold dilution for ζ -potential analysis. DLS analysis was performed using a DLS 7000 (Otsuka Electronics Co., Ltd., Osaka, Japan) at 25 °C. The light source was a He–Ne laser (630 nm) set at an angle of 45°. Experimental data were analyzed using the NNLS algorithm provided by the manufacturer. ζ -Potential analysis was performed using the same instrument.

CD spectra were measured using a J-720 spectropolarimeter (JASCO Applied Sciences, Halifax, Canada) at 25 °C. The data were obtained using a 0.1 cm path length cell at a scan speed of 20 nm/min.

Protein Loading Assay. The OVA NP dispersion was centrifuged at 15 000 \times g for 5 min. The supernatant was analyzed by gel permeation chromatography using a Superdex 200 column (GE Healthcare, Piscataway, NJ). The absorbance of the eluate was monitored at 280 nm. The concentration of OVA in the supernatant was determined from the calibration curve of the intact OVA. This concentration is for the OVA not encapsulated in the carrier (remaining OVA). The encapsulation efficiency (EE) of OVA was estimated from the following equation:

$$\text{EE(\%)} = (\text{total OVA} - \text{remaining OVA}) / \text{total OVA} \times 100$$

As for hB-Gdn-den, excitation spectra (λ_{em} 450 nm) and fluorescence spectra (λ_{ex} 380 nm) of the supernatants were measured using a RF-5300PC (Shimadzu, Kyoto, Japan). The EE was estimated using a similar equation to that shown above.

Degradation Assay. The OVA NP prepared using hB-Gdn-den (0.1 mg) remaining after the centrifugation was resuspended in 0.1 mL of trypsin solution (20 μ g/mL in phosphate buffer, pH 7.5). After 1 h at 37 °C, the sample solution (20 μ L) was analyzed by SDS-PAGE. The gel was stained with Quick-CBB (Wako Pure Chemical Industries, Ltd., Osaka, Japan) according to the manufacturer's instructions. Intact OVA, denatured OVA, and the OVA NP prepared using Gdn-den were used as controls.

Preparation of F-OVA NPs Using Dendrimers. F-OVA was prepared by reacting OVA with 20 equiv of fluorescein isothiocyanate (13 mmol/L dimethyl sulfoxide solution) in 50 mmol/L borate buffer (pH 8.0) in the dark at room temperature for 3 h. The reaction mixture was purified on a Sephadex column (Nap-25, GE Healthcare) using 0.5 mmol/L phosphate buffer (pH 7.5) as the eluent. Fluorescent OVA was diluted with nonlabeled OVA until the fluorescent OVA volume fraction decreased to 10%. The concentrations of OVA and the fluorescent dye were estimated from the Bradford protein assay (Wako Pure Chemical Industries, Ltd.) and UV–

vis spectroscopy using a UV-1650PC (Shimadzu), respectively. Equal volumes of an aqueous solution of G4-hB-Gdn or G4-Gdn (1.13 and 9.0 $\mu\text{mol/L}$) and the F-OVA solution (200 $\mu\text{g/mL}$, 4.5 $\mu\text{mol/L}$) in 0.5 mmol/L phosphate buffer (pH 7.5) were mixed together. The solution was heated at 80 $^{\circ}\text{C}$ for 30 min, then centrifuged (15 000 $\times g$, 20 min), and the residue was resuspended in EMEM.

Cell Association. For the microscopic assay, RAW 264 cells (1.5×10^5 cells) were cultured on a round glass-bottom dish (ϕ 14 mm, uncoated) overnight. The cells were washed with phosphate-buffered saline and EMEM without serum. Then, sample solutions (300 μL) were added and the dishes were incubated. After 1 h, cells were washed with phosphate-buffered saline and then treated with 0.2% Trypan blue for 3 min. The cells were washed with phosphate-buffered saline again, and observed by confocal laser scanning microscopy (Fluoview FV10i, Olympus, Tokyo, Japan).

■ ASSOCIATED CONTENT

■ Supporting Information

NMR spectrum of Gdn-den (Figure S1), TEM images of the complex of OVA and hB-Gdn-den (before heating), the OVA NPs prepared using Gdn-den and the F-OVA NPs prepared using hB-Gdn-den (Figures S2, S3, and S6), DLS and ζ -potential analyses of the OVA NPs prepared using Gdn-den (Figure S4), and SDS-PAGE of the OVA NPs prepared using Gdn-den after treatment with trypsin (Figure S5) are shown. The Supporting Information is available free of charge on the ACS Publications website at DOI: 10.1021/acs.bioconjchem.5b00325.

■ AUTHOR INFORMATION

Corresponding Authors

*E-mail: kojima@chem.osakafu-u.ac.jp. Tel.: +81 72 254 8190. Fax: +81 72 254 8190.

*E-mail: tanaka@kit.ac.jp. Tel.: +81 75 724 7861. Fax: +81 75 724 7861.

Notes

The authors declare no competing financial interest.

■ ACKNOWLEDGMENTS

This work was supported in part by a Grant-in-Aid from the Japan Society for the Promotion of Science for Scientific Research (C) (No. 26410227).

■ REFERENCES

- (1) Gombotz, W. R., and Pettit, D. K. (1995) Biodegradable polymers for protein and peptide drug delivery. *Bioconjugate Chem.* 6, 332–351.
- (2) Torchilin, V. P., and Lukyanov, A. N. (2003) Peptide and protein drug delivery to and into tumors: challenges and solutions. *Drug Discovery Today* 8, 259–266.
- (3) Lu, Y., Sun, W., and Gu, Z. (2014) Stimuli-responsive nanomaterials for therapeutic protein delivery. *J. Controlled Release* 194, 1–19.
- (4) Mellman, I., Coukos, G., and Dranoff, G. (2011) Cancer immunotherapy comes of age. *Nature* 480, 480–489.
- (5) Rosenberg, S. A., Yang, J. C., and Restifo, N. P. (2004) Cancer immunotherapy: moving beyond current vaccines. *Nat. Med.* 10, 909–915.
- (6) Mäe, M., and Langel, Ü. (2006) Cell-penetrating peptides as vectors for peptide, protein and oligonucleotide delivery. *Curr. Opin. Pharmacol.* 6, 509–514.
- (7) Wadia, J. S., and Dowdy, S. F. (2005) Transmembrane delivery of protein and peptide drugs by TAT-mediated transduction in the treatment of cancer. *Adv. Drug Delivery Rev.* 57, 579–596.
- (8) Kabanov, A. V., and Vinogradov, S. V. (2009) Nanogels as pharmaceutical carriers: finite networks of infinite capabilities. *Angew. Chem., Int. Ed.* 48, 5418–5429.
- (9) Lee, C. C., MacKay, J. A., Fréchet, J. M., and Szoka, F. C. (2005) Designing dendrimers for biological applications. *Nat. Biotechnol.* 23, 1517–1526.
- (10) Svenson, S., and Tomalia, D. A. (2005) Dendrimers in biomedical applications—reflections on the field. *Adv. Drug Delivery Rev.* 57, 2106–2129.
- (11) Kojima, C. (2010) Design of stimuli-responsive dendrimers. *Expert Opin. Drug Delivery* 7 (3), 307–319.
- (12) Astruc, D., Boisselier, E., and Ornelas, C. (2010) Dendrimers designed for functions: from physical, photophysical, and supramolecular properties to applications in sensing, catalysis, molecular electronics, photonics, and nanomedicine. *Chem. Rev.* 110, 1857–1959.
- (13) Crespo, L., Sanclimens, G., Pons, M., Giral, E., Royo, M., and Albericio, F. (2005) Peptide and amide bond-containing dendrimers. *Chem. Rev.* 105, 1663–1682.
- (14) Sadler, K., and Tam, J. P. (2002) Peptide dendrimers: applications and synthesis. *Rev. Mol. Biotechnol.* 90, 195–229.
- (15) Zhang, X., Zhao, J., Wen, Y., Zhu, C., Yang, J., and Yao, F. (2013) Carboxymethyl chitosan-poly(amidoamine) dendrimer core-shell nanoparticles for intracellular lysozyme delivery. *Carbohydr. Polym.* 98, 1326–1334.
- (16) Okuro, K., Kinbara, K., Tsumoto, K., Ishii, N., and Aida, T. (2009) Molecular glues carrying multiple guanidinium ion pendants via an oligoether spacer: stabilization of microtubules against depolymerization. *J. Am. Chem. Soc.* 131, 1626–1627.
- (17) Choi, J. S., Nam, K., Park, J. Y., Kim, J. B., Lee, J. K., and Park, J. S. (2004) Enhanced transfection efficiency of PAMAM dendrimer by surface modification with L-arginine. *J. Controlled Release* 99, 445–456.
- (18) Liu, C., Liu, X., Rocchi, P., Qu, F., Iovanna, J. L., and Peng, L. (2014) Arginine-terminated generation 4 PAMAM dendrimer as an effective nanovector for functional siRNA delivery in vitro and in vivo. *Bioconjugate Chem.* 25, 521–532.
- (19) Tanaka, N., Morimoto, Y., Noguchi, Y., Tada, T., Waku, T., Kunugi, S., Morii, T., Lee, Y., Konno, T., and Takahashi, N. (2011) The mechanism of fibril formation of a non-inhibitory serpin ovalbumin revealed by the identification of amyloidogenic core regions. *J. Biol. Chem.* 286, 5884–5894.
- (20) Wells, N. J., Basso, A., and Bradley, M. (1998) Solid-phase dendrimer synthesis. *Biopolymers* 47, 381–396.
- (21) Giehm, L., Christensen, C., Boas, U., Heegaard, P. M., and Otzen, D. E. (2008) Dendrimers destabilize proteins in a generation-dependent manner involving electrostatic interactions. *Biopolymers* 89, 522–529.
- (22) Wang, D., and Imae, T. (2004) Fluorescence emission from dendrimers and its pH dependence. *J. Am. Chem. Soc.* 126, 13204–13205.
- (23) Gratton, S. E. A., Ropp, P. A., Pohlhaus, P. D., Luft, J. C., Madden, V. J., Napier, M. E., and DeSimone, J. M. (2008) The effect of particle design on cellular internalization pathways. *Proc. Natl. Acad. Sci. U. S. A.* 105, 11613–11618.
- (24) Hamodrakas, S. J. (2011) Protein aggregation and amyloid fibril formation prediction software from primary sequence: towards controlling the formation of bacterial inclusion bodies. *FEBS J.* 278, 2428–2435.
- (25) Schneider, C. P., Shukla, D., and Trout, B. L. (2011) Effects of solute-solute interactions on protein stability studied using various counterions and dendrimers. *PLoS One* 6 (11), e27665.